High-resolution mass spectrometry unveils the molecular changes of ovalbumin induced by heating and their influence on IgE binding capacity

Mehdi Cherkaoui, Dominique Tessier, Virginie Lollier, Colette Larré, Chantal Brossard, Wieneke Dijk, Hélène Rogniaux

▶ **To cite this version:**

Mehdi Cherkaoui, Dominique Tessier, Virginie Lollier, Colette Larré, Chantal Brossard, et al.. High-resolution mass spectrometry unveils the molecular changes of ovalbumin induced by heating and their influence on IgE binding capacity. Food Chemistry, 2022, 395, pp.133624. 10.1016/j.foodchem.2022.133624 . hal-03717804

HAL Id: hal-03717804
https://hal.inrae.fr/hal-03717804v1

Submitted on 8 Jul 2022

HAL is a multi-disciplinary open access archive for the deposit and dissemination of scientific research documents, whether they are published or not. The documents may come from teaching and research institutions in France or abroad, or from public or private research centers.

L'archive ouverte pluridisciplinaire **HAL**, est destinée au dépôt et à la diffusion de documents scientifiques de niveau recherche, publiés ou non, émanant des établissements d'enseignement et de recherche français ou étrangers, des laboratoires publics ou privés.

Distributed under a Creative Commons Attribution - NonCommercial - NoDerivatives 4.0 International License

Journal Pre-proofs

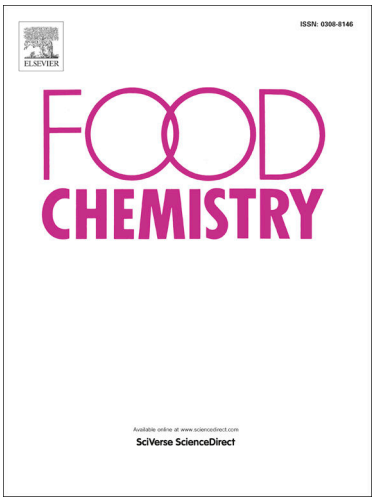

High-resolution mass spectrometry unveils the molecular changes of ovalbumin induced by heating and their influence on IgE binding capacity

Mehdi Cherkaoui, Dominique Tessier, Virginie Lollier, Colette Larre, Chantal Brossard, Wieneke Dijk, Hélène Rogniaux

PII: S0308-8146(22)01586-2
DOI: https://doi.org/10.1016/j.foodchem.2022.133624
Reference: FOCH 133624

To appear in: *Food Chemistry*

Received Date: 17 December 2021
Revised Date: 30 June 2022
Accepted Date: 30 June 2022

Please cite this article as: Cherkaoui, M., Tessier, D., Lollier, V., Larre, C., Brossard, C., Dijk, W., Rogniaux, H., High-resolution mass spectrometry unveils the molecular changes of ovalbumin induced by heating and their influence on IgE binding capacity, *Food Chemistry* (2022), doi: https://doi.org/10.1016/j.foodchem.2022.133624

This is a PDF file of an article that has undergone enhancements after acceptance, such as the addition of a cover page and metadata, and formatting for readability, but it is not yet the definitive version of record. This version will undergo additional copyediting, typesetting and review before it is published in its final form, but we are providing this version to give early visibility of the article. Please note that, during the production process, errors may be discovered which could affect the content, and all legal disclaimers that apply to the journal pertain.

© 2022 Published by Elsevier Ltd.

Title :

High-resolution mass spectrometry unveils the molecular changes of ovalbumin induced by heating and their influence on IgE binding capacity.

Authors and affiliations:

Mehdi CHERKAOUI[1,2], Dominique TESSIER[1,2], Virginie LOLLIER[1,2], Colette LARRE[1], Chantal BROSSARD[1], Wieneke DIJK[1,*], Hélène ROGNIAUX[1,2]

[1] INRAE, UR1268 BIA, F-44316 Nantes, France

[2] INRAE, PROBE research infrastructure, BIBS facility, F-44316 Nantes, France

***** corresponding author : wieneke.dijk@inrae.fr

Journal Pre-proofs

Abstract :

Ovalbumin (OVA) is a food allergen whose allergenicity is modulated by heating. We aimed to establish a molecular connection between heat-induced modifications and the modulation of the IgE binding capacity of OVA. For this, we used model samples of heat-modified OVA with increasing complexity; glycated, aggregated or glycated and aggregated. Using sera from egg-allergic individuals, we show that both aggregation and glycation strongly impacted IgE binding capacity, despite limited structural changes for glycated OVA. A molecular exploration at the amino acid level using high-resolution mass spectrometry = revealed extensive cross-linking, mostly through disulfide and dehydroprotein bridges, and moderate but significant glycation. Structural modifications affected residues located within or at a few amino acids distance of known human linear IgE epitopes, such as C121, K123, S169, K190, K207, H332 and C368. We thus unveil key amino residues implicated in the changes in IgE binding of OVA induced by heating.

Keywords : Ovalbumin, heat, aggregation, glycation, allergenicity, LC-HRMS

Journal Pre-proofs

1. Introduction

Food allergies represent a major public health issue, as world-wide prevalence and severity are increasing (Loh & Tang, 2018). Food allergens are predominantly proteins present in different food products, such as cereals, nuts, milk, eggs, fish and shellfish. One of the most common allergies is egg allergy, which affects 1.3-1.6% of children and usually develops in the first year of life (Anagnostou, 2021). A major allergen implicated in egg allergy is ovalbumin (OVA), the main protein of egg white (54%) (Urisu et al., 2015). Studies have pointed out that between 50 and 85% of egg-allergic patients can tolerate cooked or extensively heated eggs, suggesting a link between heat-induced structural modifications of egg allergens and allergenicity (Bartnikas et al., 2013; Lemon-Mulé et al., 2008).

Protein structure can be modified by thermal treatment through a loss of tertiary and secondary structures, native disulfide bond cleavage, and the random apparition of new disulfide bonds after cooling; a modification seen especially with globular proteins such as OVA (Davis & Williams, 1998; Nicolai & Durand, 2013). Indeed, the formation of the characteristic white, gel-like structure upon egg heating is the result of a progressive denaturation and aggregation of egg white proteins, including OVA (Mine, 1995; Urisu et al., 2015). Following heating, proteins can also become glycated when sugars are present in the medium through the Maillard's reaction. In the Maillard's reaction, reducing sugars react with the side chains of amino acids to form Schiff's bases, which through so-called molecular "Amadori" rearrangements lead to the formation of Advanced Glycation End products (AGEs) in a free or protein-conjugated form (Hellwig & Henle, 2014).

Several studies have investigated the impact of heat-induced glycation and aggregation on OVA allergenicity. The heat-induced glycation of OVA under dry-thermal processing conditions or under wet-thermal conditions significantly lowered the IgE binding capacity of OVA, as determined using sera from egg-allergic patients (Jiménez-Saiz et al., 2011; Liao et al., 2018) or from OVA-sensitized rabbits (Ma et al., 2013). Similar to heat-induced glycation, the progressive heat-induced aggregation of OVA seems to lower OVA allergenicity. Mice studies have shown that OVA aggregation reduces both allergy sensitization and elicitation in mice and reduces the IgE binding capacity of OVA (Claude et al., 2016; Claude et al., 2017; Jiménez-Saiz et al., 2011). There is however a lack of studies that establish a precise link between allergenicity and the heat-induced structural modifications of OVA, and especially the changes at the molecular level.

Tandem mass spectrometry (MS/MS) coupled to liquid chromatography has become a method of choice for characterizing the molecular structure of proteins, and identifying and quantifying proteins in complex biological samples for at least 20 years. However, the identification of post-translational modifications (PTMs) still remains a challenge. In a food context, chemical modifications of proteins are catalyzed by cooking, freezing, drying or storage and depend on the composition of the food matrix (presence of sugars, lipids and different proteins) (Feeney, 1982). When proteins are heated in the presence of sugar (a common process in food industry), protein groups targeted by the Maillard's reaction – such as N-terminal alpha-amino groups, epsilon-amino groups of lysine, and guanidine of arginine – get modified, and those modifications can be easily detected in MS/MS spectra (McKerchar et al., 2019; Tagami et al., 2000). Indeed, using high-resolution mass spectrometry, several studies have deciphered the glycation profile of model food proteins such as lactoglobulin from cow's milk or

ovalbumin from hen's eggs (Chen et al., 2018; Chen et al., 2012; Liao et al., 2018; Wang et al., 2020; Yang et al., 2019). These examples confirm the relevance of mass spectrometry for extensive characterization of food proteins, including their modifications (Arena et al., 2017).

Cross-link proteomics is a specific, emerging field in proteomics that allows the investigation of protein-protein interactions at a molecular level. Recently, several bioinformatic software were released or updated with the aim of deciphering complex spectra of cross-linked peptides. These new software have notably enabled the proteomics community to analyse and identify native protein cross-links via mass spectrometry at a proteome scale (Lu et al., 2015). Although the main use of these programs is in the health sector, these recent advances in data interpretation are also perfectly suited to food proteins – provided knowing the bridges upstream of the analysis – and are particularly interesting in that context, as protein cross-links are common and diverse in processed foods (McKerchar et al., 2019). The analysis of food proteomics data by these new methods will likely open the gates for detailed studies on the impact of food processing on food quality and safety. Despite the rise of cross-link proteomics approaches and adapted bioinformatics tools, there is still a lack of analyses and studies of food products using these approaches. This study aims to fill this gap by using OVA as a simplified food model.

In the present study, we mobilized the latest methodologies in tandem mass spectrometry and cross-link proteomics to decipher the heat-induced structural changes of OVA in the presence or absence of sugar. Our objective was to better understand how these structural changes could lead to a modulation of the IgE binding of OVA, depending on the process it has undergone. We thus studied different OVA model samples with an increasing level of complexity: native OVA; OVA heated under dry conditions at 55 °C, without or with glucose supplementation; and OVA heated in wet conditions at 80 °C, without or with glucose supplementation. We used glucose to promote glycation, as it is the main monosaccharide present in food preparations, although it is not the most reactive reducing sugar of the Maillard's reaction (Chen et al., 2018). We specifically focused on the identification of several Maillard's reaction-induced adducts and amino acid cross-links, as these modifications are particularly frequent in food processing but remain poorly characterized (McKerchar et al., 2019; Soboleva et al., 2017). Our results show an extensive modification of the OVA molecular structure following the different heating processes, through the formation of new cross-links and glycation of many residues. This paper provides a map of the structural changes and discusses their possible link to the modulation of OVA allergenicity.

Journal Pre-proofs

2. Materials and methods

2.1. Sera from egg-allergic patients

Sera from 9 egg-allergic children with OVA-specific IgE were selected for this study (see Supplemental Table 1). The sera belong to a registered sera collection from multiple clinical studies obtained with the informed consent of patients or their caregivers (DC-2008-809 of INRAE, UR1268 BIA Biopolymères, Interactions, Assemblages, Nantes, France) and were stored at -80 °C until use.

2.2. Protein preparation and characterization of OVA aggregates

2.2.1. Protein preparation

OVA purified from egg white with a purity of approximately 87% was kindly provided by INRAE, UMR 1253 "Science et Technologie du Lait et de l'Œuf" (STLO, Rennes, France). To obtain glycated but not aggregated OVA, OVA solutions were prepared at 20 mg/mL in 0.03 M NaCl, pH 9 in the presence or absence of 20 mg/mL of glucose. After lyophilization, the samples were heated for 24 or 72 hours at 55 °C in a 65% humidity-controlled environment using a saturated potassium iodide solution. These samples are referred to as OVA-D-H-55-24h (heated, 24h), OVA-D-HG-55-24h (heated, glycated, 24h), OVA-D-H-55-72h (heated, 72h) and OVA-D-HG-55-72h (heated, glycated, 72h). To obtain aggregated and glycated OVA, OVA solutions were prepared at 20 mg/mL in 0.03 M NaCl, pH 9 in the presence or absence of glucose (20 mg/mL) and were heated for 6 h at 80 °C in a temperature-controlled water bath to form aggregates. These samples are referred to as OVA-W-H-80-6h (aggregated) and OVA-W-HG-80-6h (aggregated, glycated). A non-aggregated OVA solution (OVA-N) was prepared by solubilizing at 20 mg/mL in 0.03M NaCl, pH 9. Aliquots were stored at −20 °C until further use.

2.2.2. SDS-PAGE

OVA-N, OVA-D-H-55-24h, OVA-D-HG-55-24h, OVA-D-H-55-72h, OVA-D-HG-55-72h, OVA-W-H-80-6h, and OVA-W-HG-80-6h were diluted at 0.167 mg/mL in Laemmli sample buffer (Bio-Rad Laboratories, France) and reduced or not by the addition of DTT (1X) and an incubation for 5 minutes at 95 °C. Fifteen µL of each sample (2.5 µg of protein/well) was loaded on a Mini-Protean TGX Precast 4-20% gel using a Mini-Protean Tetra Cell system (Bio-Rad Laboratories). A voltage of 100V was applied during 90 minutes. After migration, proteins were revealed by staining with Coomassie Blue. In order to eliminate background coloration, the gels were rinsed with distilled water before scanning (Image Scanner iii, GE Healthcare, Souffelweyersheim, France).

2.2.3. Size distribution

Particle size measurements were performed at room temperature and in triplicate. The size distributions of native and glycated OVA solutions were determined by dynamic light scattering on a Zetasizer Nano ZS (Malvern Instruments, UK), using the following refractive indexes: 1.45 for the proteins and 1.33 for the continuous phase. Samples were diluted to 10 mg/mL prior to analysis, filled into a cuvette and placed into the chamber of the Zeta sizer.

2.3. Immuno-assays on native and modified OVA

2.3.1. Dot-Blot

Increasing amounts of each OVA sample were spotted on a nitrocellulose membrane (0.2 mm, Sartorius, Germany) corresponding to 0.1, 0.5, 1 and 2 µg of protein. The membrane was then dried for 30 min at 37 °C and saturated with 4% polyvinylpyrrolidone (PVP) in Phosphate Buffered Saline (PBS; 137mM sodium chloride, 10mM phosphate, 2.7mM potassium chloride; pH 7.4), Tween 0.1% (PBS-T) for 4 h at room temperature before incubation with human sera (Supplemental Table 1) as previously described (Lupi et al., 2013). Pooled sera were prepared at a 1:25 dilution in 4% PVP in PBS-T and incubated overnight at room temperature. An anti-human IgE secondary antibody (Southern Biotech, 9205-05) was used at 1/500000 dilution in 4% PVP in PBS-T for 2 h at room temperature. The chemiluminescent substrate used for revelation was the Western Bright™ Quantum chemiluminescence HRP substrate (ADVANSTA-K12042-D20, Menlo Park, USA), and a Fuji Las3000 (Fujifilm, France) camera was used for detection.

2.3.2. Indirect ELISA

OVA-specific IgE levels were determined using indirect fluorimetric ELISA as previously described (Claude et al., 2016) using a Biomek NXP Laboratory Automation Workstation (BECKMAN Coulter, France). 20 µL of OVA-N, OVA-D-H-55-24h, OVA-D-HG-55-24h, OVA-D-H-55-72h, OVA-D-HG-55-72h, OVA-W-H-80-6h, and OVA-W-HG-80-6h diluted to 5 µg/mL in 0.1 M sodium carbonate was coated on white NuncMaxiSorp 384 well microtiter plates (Fischer Scientific, Illkirch, France) for 2 h at room temperature. Plates were blocked with 20 µL PBS-T supplemented with Gelatin 0.5% (PBS-T-G) for 2 h at 37 °C. Next, plates were incubated with 20 µL diluted human sera (1/10 dilution in PBS-T-G) overnight at 37 °C, followed by 2 h incubation at 37 °C with 20 µL of 1/500 diluted alkaline-phosphatase-conjugated anti-human IgE (A3525, Sigma, Saint-Quentin Fallavier, France, in PBS-T-G). 4-Methylumbelliferyl phosphate was used as a substrate (Sigma, Saint-Quentin Fallavier, France). Measurements were run in triplicate. The fluorescence was measured at 440 nm (excitation 360 nm) using a Synergy HT reader (Bio-tek instruments, Colmar, France). Data from indirect ELISA were analysed using a repeated measures ANOVA with a post-hoc multiple comparison Tukey (Figure 2A)) or a Dunnett's test (Figure 2C). A statistical cut-off of $p < 0.05$ was used.

2.4. OVA structural analysis at the peptide level

2.4.1. Preparations of samples prior to LC-MS analysis

Prior to digestion, samples were diluted in ammonium bicarbonate buffer (50 mM, pH 8) at a concentration of 1 mg/mL. Then, 50 µL of each diluted sample was collected and added to 10 µL of tryspin (200 ng/µL) and 138 µL of ammonium bicarbonate 50 mM, pH 8 to reach a final protease-to-protein ratio of 1:25. In order to increase the release of tryptic peptides, 2 µL of 1% (v/v) ProteaseMAX (Promega, Madison, United States) was added to reach a final concentration of 0.01% (v/v). Samples were then incubated at 37 °C for three hours and digestion was stopped by cooling samples to -20 °C. Prior to MS analysis, all digested samples were filtered on an EMPORE C8 disk (3M, Fischer Scientific, F67403 Illkirch Cedex, France) in order to remove residual salts or large polypeptides and undigested proteins.

2.4.2. Mass spectrometry analysis

Four µL of digests of each sample was injected on the nanoLC-MS/MS system composed of a hybrid Quadrupole-Orbitrap mass spectrometer (Q Exactive HF, Thermo-Fisher Scientific ™, Bremen,

Germany) coupled to a nanoscale LC system (Ultimate U3000 RSLC system, Thermo-Fisher Scientific ™, Bremen, Germany). Tryptic peptides were separated on a reversed-phase capillary column (Acclaim PepMap ™ C18, 2 µm, 100 Å, 75 µm i.d. x 25 cm long, Thermo-Fisher Scientific ™, Bremen, Germany) using a linear gradient of: (A) 99.9% water, 0.1% trifluoroacetic acid and (B) 90% acetonitrile, 9.92% water and 0.08% formic acid. After 15 minutes of column equilibration at 4% of B, the gradient consisted of a linear increase from 4% to 50% of B in 45 min, followed by a rapid increase to 90% of B within three minutes, which was maintained for two minutes and then decreased to 4% of B for re-equilibration of the column during 10 minutes. Peptides were eluted at a flowrate of 0,3 µL/min and ionized in nanoESI positive mode. Acquisitions were done using a data-dependent acquisition method. Full MS scans (*m/z* 400-2000) were acquired at 60K resolution and the fifteen most intense ions (with charges of 2-6) were fragmented in the HCD cell (NCE = 26). Fragments were analyzed in the Orbitrap analyzer at 30K resolution. Each sample was injected twice and after each run a wash program was engaged to reduce peptide carry-over on the column.

2.4.3. Bioinformatic treatment of MS data

The LC-MS/MS raw data were processed into mgf and mzXML formats using msConvert (*https://proteowizard.sourceforge.io/tools/msconvert.html*) prior to several databank searches. The proteomic data of the present work was included in the Pride database (http://www.proteomexchange.org/; dataset identifier: PXD030366).

2.4.4. Unmodified peptide identification

Identification of OVA peptides without modifications (except the oxidation of methionine Δm = +15.99) and other proteins than OVA, was done against a databank restricted to proteins belonging to Taxon 9031 (Gallus_gallus) extracted from SwissProt (2,297 entries, updated on 2021/02/02) by using X!Tandem pipeline v. 0.4.34 (Langella et al., 2017). Methionine oxidation was set as a variable modification and trypsin enzymatic cleavage was specified for the search with up to 3 miss-cleavage tolerance. Mass tolerance for precursors and fragments mass was set at +/-5 ppm or 5 ppm, respectively. Peptide identifications were validated by filtering the Peptide-Spectrum-Matches (PSM) with an e-value below 10^{-3}. Proteins were identified using at least two specific peptides and an e-value score below 10^{-4}.

2.4.5. Glycated peptides identification and localization of glycations

Databank search was done using X!Tandem against a databank restricted to proteins belonging to Taxon 9031 (Gallus_gallus) extracted from SwissProt (2,297 entries, updated on 2021/02/02). Five types of adducts targeting Lys (K) and Arg (R) were searched as variable modifications. Names, structures, targeted residues and mass delta induced by these adducts are listed in Supplemental Figure 2C. This first step allowed for the identification of peptides with a correct mass shift (depending on the type of glycation) and with a fragmentation profile sufficiently informative to confirm the peptide sequence. Glycated peptides (and residues) were filtered (and localized) using PTMProphet (Shteynberg et al., 2019) which is included in the TransProteomicPipeline (v6.0.0-rc15 Noctilucent). After identification, subsets of spectra attributed to a glycated OVA peptide were manually curated to confirm the presence and precisely localize the residue bearing the modification. To be considered as valid, a MS/MS spectrum needed to present at least one signature fragment of the glycation position (e.g. a b- or y-ion containing the glycated residue). An example of curated and annotated glycated peptide spectrum is shown in Supplemental Figure 3A.

2.4.6. Linked peptides identification

Cross-linked peptide identifications were done against a databank containing only the sequence of ovalbumin from SwissProt (P01012, OVAL_CHICK) using two dedicated databank search algorithms: pLink v. 2.3.9 (Chen et al., 2019) and Merox v. 2.0.1.4 (Götze et al., 2015). Briefly, mass tolerances for precursors and fragments were set at 3 ppm. Inbuilt FDR evaluation was used to filter identified peptides under a threshold of 1%. More detailed information about search parameters are available in Supplemental Table 2. A manual examination of identified MS/MS spectra was performed on all peptide sequences identified by the two software, and only unambiguous spectra (for linker positions on sequences) were conserved after this step. To be considered as unambiguous, a MS/MS spectrum needed to present at least one signature fragment of the cross-link position on both peptides (e.g. presence of several b- or y-ion containing the residues implicated in the bridge). An example of a curated and annotated cross-linked peptide spectrum is shown in Supplemental Figure 3B.

Journal Pre-proofs

3. Results & discussion

Several samples were prepared from the OVA protein purified from chicken egg white (further noted as OVA-N). Few other proteins than OVA were present as traces, as revealed by a complete proteomics analysis of the OVA samples (Supplemental Table 6). Two samples underwent 24-hour or 72-hour heating at 55 °C under dry conditions, without addition of glucose (hereafter referred to as OVA-D-H-55-24h or OVA-D-H-55-72h). In parallel, glycated samples were prepared by the addition of glucose (OVA-D-HG-55-24h and OVA-D-HG-55-72h). Finally, two samples were produced by heating OVA under wet conditions at 80 °C during 6 hours, without glucose (OVA-W-H-80-6h) or with glucose (OVA-W-HG-80-6h). The objective of the above preparations was to produce model samples of aggregated or glycated OVA, or of both aggregated and glycated OVA (*i.e.*, samples with a controlled and gradual complexity in the structural modifications induced on the OVA protein).

3.1. Heating at 80 °C induced a strong aggregation of OVA, while the addition of glucose led to glycation of OVA at both 55 °C and 80 °C

We first evaluated the effect of heating at 55 °C or 80 °C, in the presence or absence of glucose, on the molecular mass of OVA using SDS-PAGE (Figure 1A & 1B).

SDS-PAGE was performed either under non-reducing conditions (Figure 1A) or under reducing conditions (Figure 1B). Sample reduction disrupts the disulfide bridges that form between proteins. As shown in Figure 1A (lane 2), the dry heating of OVA at 55°C for 24h (or 72h, lane 4) did not have a major impact on the molecular weight of OVA (Figure 1A, lane 1), as the main band at 37 kDa (corresponding to native OVA) remained mostly unchanged. In the presence of glucose (lanes 3 and 5), the molecular weight increased slightly, suggesting that glycation had occurred. Glycated OVA had the same SDS-PAGE profile under non-reducing and reducing conditions, suggesting that the slight mass delta observed upon the addition of glucose did not originate from oxidation of the Cys residues. We conclude that no significant aggregation of OVA occurred upon heating at a temperature of 55°C, as no signal was detected in the high molecular weights (MW) region (> 100 kDa).

In contrast to dry heating, the wet heating of OVA at a higher temperature (80 °C) did result in the appearance of high MW bands at the top of the gel lanes in the SDS-PAGE profile under non-reducing conditions (Figure 1A, lanes 6 and 7), while the main band at 37 kDa strongly decreased in intensity. These observations suggest that OVA heating at 80 °C promotes aggregation. This aggregation seemed to be principally driven by the formation of new disulfide bonds, as the high MW bands seen under non-reducing conditions disappeared under reducing conditions (Figure 1B, lanes 6 and 7). The presence of residual bands at masses higher than 100 kDa in the reduced samples suggests that other amino acid cross-links, such as bonds between dehydroproteins or dityrosine (diTyr) bonds, that are not susceptible to the reducing agent were also formed (McKerchar et al., 2019), although the identity of these bridges needs to be formally established by MS analysis. Similar to the samples heated at 55 °C the presence of glucose had no major effect on the structure of OVA heated at 80 °C: the mass

profiles in SDS-PAGE are comparable between the samples heated at 80 °C without or with glucose (Figure 1A & 1B, lanes 6 and 7).

Complementary to SDS-PAGE analysis, Dynamic Light Scattering (DLS) measurements were performed on all samples (Figures 1C, 1D, 1E). DLS was used to determine the size distribution profile of OVA particles in solution. Corresponding to the SDS-PAGE observations, DLS measurements indicated no significant change in the size distribution for the samples heated at 55 °C without glucose compared to native OVA, while a slight shift towards bigger sizes was observed for glucose supplemented samples (red curves in Figures 1C and 1D), especially after 72 hours. In contrast, a net shift was observed for samples heated at 80 °C (Figure 1E). Together, these results confirm that the model samples conceived for the study, with two different heating temperatures and supplementation or not with glucose, allowed the successful generation of glycated and aggregated OVA samples, with increasing levels of complexity (aggregation or glycation only on one hand, aggregation and glycation on the other hand). A schematic representation of the different samples is proposed in Supplemental Figure 1A, compiling the knowledge from SDS-PAGE and DLS analyses regarding the structural changes of OVA at the protein level.

Further information about the structural modifications of OVA induced by heat was provided by a global analysis of tandem mass spectrometry metadata collected from the tryptic peptides generated from the different OVA samples. These data can be represented in the form of a "heatmap", in which each spot represents the mass and the chromatographic retention time of a precursor peptide selected to be fragmented by MS/MS. Heatmaps are provided for all OVA model samples in Supplemental Figure 4. In line with the data obtained using SDS-PAGE and DLS, the heatmaps showed a clear distinction of samples heated at 80°C (OVA-W-H-80-6h and OVA-W-HG-80-6h) compared to OVA-N or to samples dry-heated at 55 °C (OVA-D-H-55-24h, OVA-D-H-55-72h, OVA-D-HG-55-24h and OVA-D-HG-55-72h). The samples heated at 80 °C were more chemically complex, with precursors selected all along the gradient with deconvoluted masses comprised between 1000 and 7500 Da. This indicated a higher peptide diversity in these samples and the presence of larger peptides, reflecting the aggregation in these samples. In contrast, precursors selected for OVA-N, OVA-D-H-55-24h, OVA-D-H-55-72h, OVA-D-HG-55-24h or OVA-D-HG-55-72h were almost all eluted at the beginning of the gradient with masses between 1000 and 3500 Da. The low chemical diversity in the OVA-N sample can be explained by the fact that OVA has a serine-type endopeptidase inhibitor activity, which can inhibit trypsin digestion (Donovan & Mapes, 1976). Indeed, a sequence coverage of around 50% was obtained for OVA-N, while a 98% coverage was obtained when OVA was treated with a reducing agent prior to trypsin digestion (and thus loses its structure; data not shown). Similarly, the chemical diversity observed for the samples heated at 80 °C can be explained by a significant loss of the OVA tertiary structure (as a result of both temperature and aggregation), which results in a more efficient hydrolysis by trypsin and a higher number of released peptides. This was confirmed by the higher peptide coverage of the OVA primary sequence for samples heated at 80 °C (wet conditions) than for samples heated at 55 °C (dry-heated) or native OVA (Supplemental Data Table 3). Moreover, deeply buried peptides such as ^{361}ADHPFLFCIK^{370} are more efficiently released in the samples heated at 80 °C (in-solution), again suggesting a significant modification of OVA's tertiary structure in these samples. Sequence coverage and peptide release is lower in samples supplemented with glucose than without glucose. As Lys and Arg are the target residues of glycation and also the sites of cleavage by trypsin,

the steric hindrance generated around these residues by glucose adducts (or Maillard's reaction products) could also explain an altered activity of trypsin.

3.2. Heat-induced structural modifications lowered the IgE binding capacity of OVA

We next determined the impact of these different structural modifications on OVA antigenicity using two complementary immunochemical methods; indirect ELISA and dot blot.

Using indirect ELISA and sera from egg-allergic patients (Supplemental Table 1), we show that the dry heating of OVA (55 °C) for 24h or 72h modestly increased the IgE binding capacity of OVA, possibly due to a partial unfolding of the tertiary protein structure following heating (Mine, 1995) (Figure 2A, OVA-D-H-55-24h & OVA-D-H-55-72h). In contrast, the glycation of OVA using dry heating moderately but significantly reduced the IgE binding capacity of sera from egg-allergic patients (Figure 2A, OVA-D-HG-55-24h & OVA-D-HG-55-72h). No significant differences were observed between 24h and 72h of glycation (Figure 2A). This reduction in the IgE binding capacity of OVA upon glycation was confirmed using dot blot and a pool of sera from egg-allergic patients (Figure 2B) and is in line with observations from other studies (Jiménez-Saiz et al., 2011; Ma et al., 2013).

In contrast to the moderate changes in IgE binding capacity of OVA glycation, the aggregation of OVA following heating at 80 °C (wet heating) led to a much stronger reduction of OVA's IgE binding capacity, as shown using indirect ELISA with sera from egg-allergic patients (Figure 2C). We did not observe any impact of glycation in addition to that of heat-induced aggregation on IgE binding capacity using indirect ELISA, suggesting that the impact of glycation on allergenicity is relatively modest in heat-aggregated OVA (Figure 2C). We did, however, observe a modest additional reduction in IgE binding capacity using dot blot (Figure 2D). The reason for this apparent discrepancy remains unclear, but is likely to be linked to the methodological differences between the two techniques (plate coating *vs.* dotting on membrane). A previous study also indicated that a pre-heating of OVA at 60 °C – inducing partial unfolding – followed by glycation at 50 °C (dry heat) modestly lowers IgE binding capacity compared to pre-heating at lower temperatures such as 20 °C or 40 °C (Liao et al., 2018). Overall, our results confirm the link between heat-induced structural modifications of OVA and a reduction in OVA antigenicity. We show that OVA glycation has a moderate impact on IgE binding capacity, whereas the aggregation of OVA has a stronger impact.

3.3. Glycation of OVA takes place primarily on exposed residues

As shown above, a moderate yet significant decrease in OVA antigenicity was observed following heat-induced glycation. In order to correlate this behaviour to structural changes of the protein at the amino acid level, we next attempted to specifically identify glycated peptides and to map the glycation sites of the different OVA samples.

We used X!Tandem and PTMProphet to automatically identify the glycated OVA peptides. As described in detail in the Material and Methods section, hit spectra were manually curated to confirm the precise localization of modified residues. We specifically searched for five types of modifications: glucose substitution (+162.053 Da) and four well-described AGEs: CarboxyMethylLysine (CML ; +58.006

Da), CarboxyEthylLysine (CEL ; +72.021 Da), pyrraline (+108.021 Da) and Arg-pyrimidine (+80.085 Da). A full list of the identified glycated peptides and the position of the modified residues is available in Supplemental Data Table 4. Figure 3 provides a schematized view of the glycation sites mapped on the OVA sequence for all heated samples. As expected, no glycated peptides were identified in the samples that had no glucose supplementation, *i.e.*, the following samples: OVA-N, dry-heated OVA without glucose supplementation (OVA-D-H-55-24h & OVA-D-H-55-72h) and aggregated OVA (OVA-W-H-80-6h). In contrast, a significant number of spectra were found in the samples that were heated at 55 °C, and which were essentially glycated (dry heated, OVA-D-HG-55-24h (28 spectra) and OVA-D-HG-55-72h (44 spectra)). The highest number of spectra (134 spectra) attributed to glycated peptides was identified in the sample heated at 80 °C with glucose (OVA-W-HG-80-6h), which is thus aggregated and glycated. The residues K93 and K207 were the main amino acids targeted for glycation in all samples, in accordance with literature (Liao et al., 2018; Tu et al., 2017; Wang et al., 2020). These residues are located in two of the most hydrophilic and exposed areas of OVA tertiary structure (data not shown, see *https://www.rcsb.org/3d-sequence/1OVA*) making them ideal targets for glycation. Interestingly, all glycated residues identified in dry-heated OVA samples supplemented with glucose (OVA-D-HG-55-24h & OVA-D-HG-55-72h) are located in hydrophilic areas of the OVA tertiary structure. In contrast, the glycation profile of the samples heated at 80 °C (OVA-W-HG-80-6h) showed a much larger diversity of glycated residues, with glycation sites spread all along the OVA primary sequence including some deeply buried areas (see *https://www.rcsb.org/3d-sequence/1OVA*). This confirms the limited level of OVA tertiary structure denaturation in moderately heated samples at 55 °C, and a much stronger impact on the OVA structure induced at 80 °C, the latter condition probably allowing the exposition of residues localized in hydrophobic (and buried) areas of the native structure. We also identified more AGEs in this sample, although only glucose and pyrraline adducts were unambiguously identified in mass spectrometry data, with most peptides substituted by one glucose unit. This indicates that the Maillard's reaction was not sufficiently advanced in all samples to cause the apparition of other AGEs. In this study, all MS/MS spectra were carefully and manually curated to list the glycated peptides. This manual curation of glycation data yields results with high confidence, as compared to unreviewed software-based assignments. For example, we rejected all proposed hits that had no fragments on the spectrum clearly attesting the position of glycation. Consequently, the number of glycated residues remains modest as compared to other studies (Liao et al., 2018; Yang et al., 2019), which are otherwise comparable regarding the preparation of OVA samples. To allow the reader to examine those data, raw MS files have been placed in a public repository (PRIDE, PXD030366).

3.4. Glycation hotspots of heated OVA lay in proximity to human IgE epitopes

In data dependent analyses (*i.e.*, the acquisition method used in our work), the number of spectra assigned to one peptide ("spectral count") can provide an estimation of the peptide's relative abundance even though it is not directly proportional to the absolute amount of the peptide in the sample (Liu et al., 2004). By examining the numbers of spectra attributed to each glycated residue, we thus defined "hotspots" of glycation, meaning that these residues were identified as glycated in a high number of spectra. The hotspots are localized around K93 and K207, two of the most exposed residues (Figure 3). Interestingly, the hotspot around K207 was shared among all samples supplemented with glucose and was localized in close proximity to one of the known human linear IgE epitopes : ^{188}AF**K**DEDTQAMP^{198} (Benedé et al., 2014). For OVA heated at 80 °C with glucose (OVA-W-HG-80-6h),

the glycated residues R127, K190 or K370 were also identified, an interesting observation as they are respectively located inside of the following linear IgE epitopes : ^{125}LY**R**GGLEPIN^{134}, ^{188}AF**K**DEDTQAMP^{198} and ^{370}**K**HIATNAVLFFGRCVS^{385} (Benedé et al., 2014) (Figure 3). By modifying these three different epitopes, we hypothesize that glycation may contribute to the moderate reduction of allergenicity observed in this study or previous ones (Jiménez-Saiz et al., 2011; Liao et al., 2018).

3.5. Aggregation is mainly driven by the formation of disulfide bridges and bonds between dehydroproteins

Our results and previous studies (Claude et al., 2017) have established that the heat-induced aggregation of OVA strongly lowers its allergenicity. To go deeper into the molecular explanation for these changes, we used a cross-link proteomics approach to identify the bridges formed upon heating either in moderate conditions (55 °C) or at higher temperature (80 °C).

Native OVA (OVA-N) was taken as a control of the initial cross-link status. Tryptic digestion was performed under non-reducing conditions to preserve disulfide bridges during the preparation step. Notably, the fragmentation technique employed in this study, so called “HCD” (standing for “higher-energy collisional dissociation”), has been shown to preserve disulfide bonds (Cui et al., 2019). In the present work, fragments produced by HCD were measured at a resolving power of 30k in an orbitrap mass analyzer, with an extended *m/z* range (up to 4000 *m/z*). The combination of both technical features (*i.e.*, HCD and orbitrap) led to MS/MS spectra containing helpful information for the identification of bridged peptides, including peptides with high *m/z* ratio and/or high charges, and the presence of highly charged fragments attributed to both peptides involved in the bridge. Dedicated software, such as pLink and MEROX, have been developed to decipher complex HCD fragmentation spectra of cross-linked peptides and were used in this study. However, these tools suffer from a high rate of false positive identifications as evidenced by a recent study (Beveridge et al., 2020). This report led us to carefully curate the hits proposed by MEROX and/or pLink before validation and biological interpretation. A full list of the validated aggregated peptides with positions of bridged residues is available in Supplementary Table 5.

Following this approach, we identified several cross-linked peptides (*i.e.*, two different peptides linked by two of their amino acids, Supplemental Figure 4B) connected by different linkers (listed in Supplemental Figure 2B). These linkers are expected to form spontaneously during heating and/or the Maillard’s reaction. Aggregation sites identified by our analysis are listed in Table 2 and are represented in Figure 4. First of all, no cross-linked peptides were detected in native OVA (OVA-N) sample. We assume that the disulfide bridge reported in OVA in its native state (data not shown, see *https://www.rcsb.org/3d-sequence/1OVA*) was not identified in our study, probably due to the poor trypsin digestion of the native OVA sample. In line with other structural data, only few cross-linked peptides were identified in the samples heated at 55 °C (OVA-D-H-55-24h & OVA-D-H-55-72h)). Indeed, only 15 and 5 unique peptide bridges, respectively, were identified in those samples not supplemented with glucose heated for 24 and 72 hours. Glucose supplementation further reduced the number of identified cross-links to 5 and 2 unique peptide bridges after 24 or 72 hours of heating, respectively. In contrast, for OVA samples heated at 80 °C (OVA-W-H-80-6h & OVA-W-HG-80-6h), 24 unique peptide bridges were identified without glucose supplementation and 27 with glucose

supplementation. These results indicate a strong diversity of cross-bridges and suggest that glycation did not significantly affect the cross-linking in these samples.

In the samples heated at 55 °C, a limited number of heat-induced individual disulfide bridges was identified, probably due to the limited accessibility of other Cys residues to form bridges. In these samples, the Cys residue most involved in the formation of disulfide bridges was C121, which is a highly exposed Cys on the OVA surface, whereas the most prevalent peptide bridge was a lysinoalanine bridge between K264 and S270. Interestingly, we noticed that the addition of glucose had a clear effect on the aggregation sites. Without glucose supplementation, aggregation takes place predominantly on lysine residues via lysinoalanine bridges. In contrast, with glucose supplementation these bridges are less frequent or even lost (e.g. the lysinoalanine bridge between S222 and K207). As K207 is the most glycated residue in our study, we suspect that a competition between aggregation and glycation exists on exposed residues, as both modifications target the same residue. Another example that illustrates this possible competition is K190, which was identified in previous studies as one of the preferential targets of glycation (Liao et al., 2018; Wang et al., 2020). We did not find any peptide containing this glycated residue, but did find several cross-linked peptides at this residue (OVA-D-HG-55-72h).

For the samples heated at 80 °C, the majority of the bridges identified are disulfide bridges involving two Cys residues (Table 2). Our results show that all Cys of the OVA sequence – including the most buried Cys (C31, C368, C383) – are linked to another Cys, with C121 and C368 being the Cys residues most involved in disulfide bridge formation (as identified with at least 4 MS/MS spectra), which are respectively one of the most and one of the least exposed residues. Our SDS-PAGE profiles showed the continued presence of low intensity bands at high molecular weights for samples heated at 80 °C under reducing conditions (Figure 1), suggesting the presence of cross-links insensitive to the reducing agent. In agreement with this, a significant number of spectra were attributed to peptides arising from bridges between dehydroproteins (with a prevalence of lysinoalanine bridges, followed by lanthionine and histidinoalanine). The rest of the identified spectra were attributed to dityrosine and Maillard's reaction-induced cross-links. As indicated by the analysis of the glycation sites (see above), the Maillard's reaction was not very advanced in these samples but apparently sufficient to initiate cross-links. Cross-links induced by the Maillard's reaction were also identified in samples without glucose supplementation, possibly due to the presence of residual sugars after OVA purification, as egg white contains a small amount of sugars (about 0,7% of carbohydrate).

3.6. Aggregation hotspots of heated OVA are localized in proximity to human linear IgE epitopes

The number of spectra attributed to cross-linked OVA peptides was used to determine the aggregation hotspots in each sample (Figure 4).

For dry-heated samples not supplemented with glucose (OVA-D-H-55-24h and OVA-D-H-55-72h), many heat-induced bridges form in a region from amino acid K182 to K278, a significant number of which involve the residue K190 that is part of the linear IgE epitope: ^{188}AF**K**DEDTQAMP^{198}. For dry-heated samples supplemented with glucose (OVA-D-HG-55-24h and OVA-D-HG-55-72h), three hotspots were identified. A first one around residue C121, a second one involves residues S169 and K190 and a third one involves residues S264 and S270. The cross-linking of residues S169 and K190,

which are constitutive of the following IgE epitopes: ^{159}RNVLQPSSVD**S**QTA^{172} and ^{188}AF**K**DEDTQAMP^{198}, probably contributes to the reduced IgE binding capacity observed in dry-heated samples supplemented with glucose. An interesting observation is that less cross-linked peptides were identified in dry-heated samples supplemented with glucose. We believe that this might be explained by a kinetic competition between aggregation and the Maillard's reaction, as the majority of identified cross-links were lysinoalanine bridges involving Lys residues, which are also the targets of Maillard's reaction.

For wet-heated samples (OVA-W-H-80-6h, OVA-W-HG-80-6h), the SDS-PAGE and DLS profiles showed an extensive aggregation of OVA upon wet heating at 80 °C. The cross-linked peptide analysis established that the main aggregation sites in these samples are localized near human IgE linear epitopes. A first hotspot is located between Y118 and K123, which is only two amino acids residues far from the linear IgE epitope ^{125}LYRGGLEPIN^{134}. A second hotspot is located between C368 and C383 inside the most reactive C-ter linear epitope ^{370}KHIATNAVLFFGRCVS^{385} (Benedé et al., 2014). It should be noted that this epitope is deeply buried in the native OVA sequence and thus not readily accessible to IgEs in the native OVA conformation. Therefore, its modification cannot fully explain the reduction in OVA IgE binding capacity measured on wet heated samples in our study as it is probably not recognized by IgEs in OVA native conformation. However, it can be hypothesized that it will be released upon intestinal digestion and that its extensive structural modification may lower its binding capacity to IgEs, therefore contributing to the observation that extensively cooked eggs are generally better tolerated than raw eggs by egg-allergic patients (Benedé et al., 2014; Lemon-Mulé et al., 2008).

The observation that deeply buried peptides are involved in cross-links suggests that most of the conformational epitopes of OVA were lost under heating at 80 °C, which might partly explain the observed reduction in IgE binding. However, a previous study established that linear epitopes are also important for OVA allergenicity (Järvinen et al., 2007). It can be presumed that the structural modifications due to cross-links affecting residues that are surface exposed and localized near to or within human IgE linear epitopes, such as the amino acids described above, will result in steric hindrance and/or local conformational changes that may prevent the binding of IgEs to those epitopes. In this context, the bridging of residue H332 is of particular interest in wet-heated samples (even if it was not identified inside an aggregation hotspot), as this amino acid is located within the well-established B- and T-cell epitope of OVA ^{323}KISQAVHAA**H**AEINEAG^{339} (Benedé et al., 2014). Altogether, the identified peptide cross-links provide a possible explanation for the reduced IgE binding capacity (and resulting allergenicity) of OVA after heating. This reduction can be explained either through the loss of conformational epitopes, following extensive conformational loss of OVA, or through extensive modifications at the vicinity of linear epitopes that may hinder the binding of IgEs.

Previous studies have identified the Maillard's reaction as the responsible reaction for carcinogenic compound formation in food (Hellwig & Henle, 2014; Schröter & Höhn, 2019). Our results suggest that the early Maillard's reaction can also have beneficial health effects by modulating allergen structure, which – in the case of OVA – leads to a reduced IgE binding capacity. In order to confirm this hypothesis, the use of bioinformatic identification tools without *a-priori* on the mass delta of the peptides would allow obtaining a more exhaustive view of the glycated residues of OVA after the Maillard's reaction. Our fine structural characterization of glycated and/or aggregated OVA is not fully exhaustive. Indeed, due to the limitations of most of the current algorithms, we had to make some *a-priori* on the mass

delta induced by the modifications (glycation or aggregation). Peptides with more complex modification patterns (e.g., aggregated and glycated peptides) are probably present in our samples, as attested by a few examples (Supplemental Figure 3C), but were not identified by the current approach as we limited the number of modifications that were searched in the same analysis in order to reduce the risk of false positive identifications. Moreover, the Maillard's reaction is a complex cascade of reactions that leads to the formation of numerous end-products that are not all well characterized. In this context, the recent development and improvement of Open Mass Search algorithms such as SpecOMS or MSFragger (David et al., 2017; Kong et al., 2017) will be of great help to further elucidate and characterize the structural modifications induced by food processes on food proteins and to fully exploit the potential of data obtained by high-resolution mass spectrometry in discovery approaches.

Journal Pre-proofs

4. Conclusion

In conclusion, in this work we provide for the first time a detailed molecular view of the glycation and aggregation status of OVA following thermal treatment using a high-resolution mass spectrometry-based approach. Our analyses show that heat-induced modifications of linear IgE epitopes are closely linked to the reduction of IgE binding capacity of OVA. Our work implicates key amino residues in the changes in IgE binding of OVA following heating, such as C121, K123, S169, K190, K207, H332 and C368. These structural changes at the amino acid level provide an explanation for the stronger impact of aggregation on IgE binding compared to glycation, but also explain why glycation lowered IgE binding capacity despite limited structural changes at the protein level. Lastly, our results highlight the promise of new generation interpretation software on high-resolution mass spectrometry-based approaches to study heat-induced modifications, including the Maillard's reaction and protein cross-linking, in food products. Quantitative analysis of native *vs* modified allergenic peptides could also extend the study and help specifying the predominance of specific aggregation hotspots.

Journal Pre-proofs

Abbreviations

AGEs : Advanced Glycation End-products
HRMS : High-Resolution Mass Spectrometry
HCD : Higher-energy Collisional Dissociation
IgE : Immunoglobulin E
MW: Molecular weight
OVA : Ovalbumin
PBS: Phosphate Buffered Saline
PBS-T: PBS containing 0,1% Tween
PBS-T-G : PBS containing 0,1% Tween and 0,5% Gelatin
PTM : Post-Translational Modification

Acknowledgements

We thank Pr. Françoise Nau, Pr. Catherine Guérin-Dubiard, and Kéra Nyemb (UMR1253 STLO, INRA Rennes, France) for providing us with purified OVA. We also thank Gilbert Deshayes for excellent technical assistance.

Funding

This work was supported by the Agence Nationale de la Recherche as part of the “DeepProt” project (ANR-18-CE45-004).

Author contribution

Conceptualization and methodology: C.L., C.B., H.R. and D.T.; Formal analysis and investigation: M.C., W.D., D.T. and V.L.,; Data curation : M.C.; Writing _original draft preparation : M.C., W.D., and H.R.; Writing-review and editing, M.C., W.D., V.L., C.L, C.B., D.T., and H.R.; Supervision : H.R. and D.T.; Funding acquisition : H.R. and D.T.
All authors have read and agreed to the published version of the manuscript.

Journal Pre-proofs

References:

Anagnostou, A. (2021). Optimizing patient care in egg allergy diagnosis and treatment. *Journal of Asthma and Allergy*, *14*, 621–628. https://doi.org/10.2147/JAA.S283307

Arena, S., Renzone, G., D'Ambrosio, C., Salzano, A. M., & Scaloni, A. (2017). Dairy products and the Maillard reaction: A promising future for extensive food characterization by integrated proteomics studies. *Food Chemistry*, *219*, 477–489. https://doi.org/10.1016/j.foodchem.2016.09.165

Bartnikas, L. M., Gurish, M. F., Burton, O. T., Leisten, S., Janssen, E., Oettgen, H. C., Beaupré, J., Lewis, C. N., Austen, K. F., Schulte, S., Hornick, J. L., Geha, R. S., & Oyoshi, M. K. (2013). Epicutaneous sensitization results in IgE-dependent intestinal mast cell expansion and food anaphylaxis. *The Journal of Allergy and Clinical Immunology*, *131*(2), 451. https://doi.org/10.1016/J.JACI.2012.11.032

Benedé, S., López-Expósito, I., López-Fandiño, R., & Molina, E. (2014). Identification of IgE-Binding Peptides in Hen Egg Ovalbumin Digested in Vitro with Human and Simulated Gastroduodenal Fluids. *Journal of Agricultural and Food Chemistry*, *62*(1), 152–158. https://doi.org/10.1021/jf404226w

Beveridge, R., Stadlmann, J., Penninger, J. M., & Mechtler, K. (2020). A synthetic peptide library for benchmarking crosslinking-mass spectrometry search engines for proteins and protein complexes. *Nature Communications*, *11*(1), 1–9. https://doi.org/10.1038/s41467-020-14608-2

Chen, Y. J., Liang, L., Liu, X. M., Labuza, T. P., & Zhou, P. (2012). Effect of fructose and glucose on glycation of β-lactoglobulin in an intermediate-moisture food model system: Analysis by liquid chromatography-mass spectrometry (LC-MS) and data-independent acquisition LC-MS (LC-MSE). *Journal of Agricultural and Food Chemistry*, *60*(42), 10674–10682. https://doi.org/10.1021/jf3027765

Chen, Y., Tu, Z. cai, Wang, H., Liu, G. xian, Liao, Z. wei, & Zhang, L. (2018). LC-Orbitrap MS analysis of the glycation modification effects of ovalbumin during freeze-drying with three reducing sugar additives. *Food Chemistry*, *268*(June), 171–178. https://doi.org/10.1016/j.foodchem.2018.06.092

Chen, Z.-L., Meng, J.-M., Cao, Y., Yin, J.-L., Fang, R.-Q., Fan, S.-B., Liu, C., Zeng, W.-F., Ding, Y.-H., Tan, D., Wu, L., Zhou, W.-J., Chi, H., Sun, R.-X., Dong, M.-Q., & He, S.-M. (2019). A high-speed search engine pLink 2 with systematic evaluation for proteome-scale identification of cross-linked peptides. *Nature Communications*, *10*(1), 3404. https://doi.org/10.1038/s41467-019-11337-z

Claude, M., Lupi, R., Bouchaud, G., Bodinier, M., Brossard, C., & Denery-Papini, S. (2016). The thermal aggregation of ovalbumin as large particles decreases its allergenicity for egg allergic patients and in a murine model. *Food Chemistry*, *203*, 136–144. https://doi.org/10.1016/j.foodchem.2016.02.054

Claude, Mathilde, Bouchaud, G., Lupi, R., Castan, L., Tranquet, O., Denery-Papini, S., Bodinier, M., & Brossard, C. (2017). How Proteins Aggregate Can Reduce Allergenicity: Comparison of Ovalbumins Heated under Opposite Electrostatic Conditions. *Journal of Agricultural and Food Chemistry*, *65*(18), 3693–3701. https://doi.org/10.1021/acs.jafc.7b00676

Cui, C., Liu, T., Chen, T., Lu, J., Casaren, I., Lima, D. B., Carvalho, P. C., Beuve, A., & Li, H. (2019). Comprehensive Identification of Protein Disulfide Bonds with Pepsin/Trypsin Digestion, Orbitrap HCD and Spectrum Identification Machine. *Journal of Proteomics*, *198*, 78. https://doi.org/10.1016/J.JPROT.2018.12.010

David, M., Fertin, G., Rogniaux, H., & Tessier, D. (2017). SpecOMS: A Full Open Modification Search Method Performing All-to-All Spectra Comparisons within Minutes. *Journal of Proteome Research*, *16*(8), 3030–3038. https://doi.org/10.1021/acs.jproteome.7b00308

Davis, P. J., & Williams, S. C. (1998). Protein modification by thermal processing. *Allergy: European Journal of Allergy and Clinical Immunology*, *53*(SUPPL. 46), 102–105. https://doi.org/10.1111/J.1398-9995.1998.TB04975.X/FORMAT/PDF

Donovan, J. W., & Mapes, C. J. (1976). A differential scanning calorimetric study of conversion of ovalbumin to S-ovalbumin in eggs. *Journal of the Science of Food and Agriculture*, *27*(2), 197–204. https://doi.org/10.1002/JSFA.2740270220/FORMAT/PDF

Feeney, R. (1982). *Chemical Modification of Food Proteins* (pp. 275–300). https://doi.org/10.1021/bk-1982-0206.ch011

Götze, M., Pettelkau, J., Fritzsche, R., Ihling, C. H., Schäfer, M., & Sinz, A. (2015). Automated assignment of MS/MS cleavable cross-links in protein 3D-structure analysis. *Journal of the American Society for Mass Spectrometry*, *26*(1), 83–97. https://doi.org/10.1007/S13361-014-1001-1

Hellwig, M., & Henle, T. (2014). Baking, Ageing, Diabetes: A Short History of the Maillard Reaction. *Angewandte Chemie - International Edition*, *53*(39), 10316–10329. https://doi.org/10.1002/anie.201308808

Järvinen, K. M., Beyer, K., Vila, L., Bardina, L., Mishoe, M., & Sampson, H. A. (2007). Specificity of IgE antibodies to sequential epitopes of hen's egg ovomucoid as a marker for persistence of egg allergy. *Allergy*, *62*(7), 758–765. https://doi.org/10.1111/J.1398-9995.2007.01332.X

Jiménez-Saiz, R., Belloque, J., Molina, E., & López-Fandiño, R. (2011). Human immunoglobulin e (IgE) binding to heated and glycated ovalbumin and ovomucoid before and after in vitro digestion. *Journal of Agricultural and Food Chemistry*, *59*(18), 10044–10051. https://doi.org/10.1021/jf2014638

Kong, A. T., Leprevost, F. V., Avtonomov, D. M., Mellacheruvu, D., & Nesvizhskii, A. I. (2017). MSFragger: ultrafast and comprehensive peptide identification in mass spectrometry–based proteomics. *Nature Methods 2017 14:5*, *14*(5), 513–520. https://doi.org/10.1038/nmeth.4256

Langella, O., Valot, B., Balliau, T., Blein-Nicolas, M., Bonhomme, L., & Zivy, M. (2017). X!TandemPipeline: A Tool to Manage Sequence Redundancy for Protein Inference and Phosphosite Identification. *Journal of Proteome Research*, *16*(2), 494–503. https://doi.org/10.1021/acs.jproteome.6b00632

Lemon-Mulé, H., Sampson, H. A., Sicherer, S. H., Shreffler, W. G., Noone, S., & Nowak-Wegrzyn, A. (2008). Immunologic changes in children with egg allergy ingesting extensively heated egg. *Journal of Allergy and Clinical Immunology*, *122*(5), 977–983. https://doi.org/10.1016/j.jaci.2008.09.007

Liao, Z. W., Ye, Y. H., Wang, H., Chen, Y., Sha, X. M., Zhang, L., Huang, T., Hu, Y. M., & Tu, Z. C. (2018). The Mechanism of Decreased IgG/IgE-Binding of Ovalbumin by Preheating Treatment Combined with Glycation Identified by Liquid Chromatography and High-Resolution Mass Spectrometry. *Journal of Agricultural and Food Chemistry*, *66*(41), 10693–10702. https://doi.org/10.1021/acs.jafc.8b04165

Liu, H., Sadygov, R. G., & Yates, J. R. (2004). A Model for Random Sampling and Estimation of Relative Protein Abundance in Shotgun Proteomics. *Analytical Chemistry*, *76*(14), 4193–4201. https://doi.org/10.1021/ac0498563

Loh, W., & Tang, M. L. K. (2018). The Epidemiology of Food Allergy in the Global Context. *International Journal of Environmental Research and Public Health*, *15*(9), 2043–2052. https://doi.org/10.3390/ijerph15092043

Lu, S., Fan, S. B., Yang, B., Li, Y. X., Meng, J. M., Wu, L., Li, P., Zhang, K., Zhang, M. J., Fu, Y., Luo, J., Sun, R. X., He, S. M., & Dong, M. Q. (2015). Mapping native disulfide bonds at a proteome scale. *Nature Methods 2015 12:4*, *12*(4), 329–331. https://doi.org/10.1038/nmeth.3283

Lupi, R., Denery-Papini, S., Rogniaux, H., Lafiandra, D., Rizzi, C., De Carli, M., Moneret-Vautrin, D. A., Masci, S., & Larré, C. (2013). How much does transgenesis affect wheat allergenicity?: Assessment in two GM lines over-expressing endogenous genes. *Journal of Proteomics*, *80*, 281–291. https://doi.org/10.1016/J.JPROT.2013.01.028

Ma, X. J., Chen, H. B., Gao, J. Y., Hu, C. Q., & Li, X. (2013). Conformation affects the potential allergenicity of ovalbumin after heating and glycation. *Food Additives & Contaminants: Part A*, *30*(10), 1684–1692. https://doi.org/10.1080/19440049.2013.822105

McKerchar, H. J., Clerens, S., Dobson, R. C. J., Dyer, J. M., Maes, E., & Gerrard, J. A. (2019). Protein-protein crosslinking in food: Proteomic characterisation methods, consequences and applications. *Trends in Food Science & Technology*, *86*, 217–229. https://doi.org/10.1016/J.TIFS.2019.02.005

Mine, Y. (1995). Recent advances in the understanding of egg white protein functionality. *Trends in Food Science and Technology*, *6*(7), 225–232. https://doi.org/10.1016/S0924-2244(00)89083-4

Nicolai, T., & Durand, D. (2013). Controlled food protein aggregation for new functionality. *Current Opinion in Colloid and Interface Science*, *18*(4), 249–256. https://doi.org/10.1016/J.COCIS.2013.03.001

Schröter, D., & Höhn, A. (2019). Role of Advanced Glycation End Products in Carcinogenesis and their Therapeutic Implications. *Current Pharmaceutical Design*, *24*(44), 5245–5251. https://doi.org/10.2174/1381612825666190130145549

Shteynberg, D. D., Deutsch, E. W., Campbell, D. S., Hoopmann, M. R., Kusebauch, U., Lee, D., Mendoza, L., Midha, M. K., Sun, Z., Whetton, A. D., & Moritz, R. L. (2019). PTMProphet: Fast and Accurate Mass Modification Localization for the Trans-Proteomic Pipeline. *Journal of Proteome Research*, *18*(12), 4262–4272. https://doi.org/10.1021/acs.jproteome.9b00205

Soboleva, A., Vikhnina, M., Grishina, T., & Frolov, A. (2017). Probing Protein Glycation by Chromatography and Mass Spectrometry: Analysis of Glycation Adducts. *International Journal of Molecular Sciences*, *18*(12), 2557. https://doi.org/10.3390/ijms18122557

Tagami, U., Akashi, S., Mizukoshi, T., Suzuki, E., & Hirayama, K. (2000). Structural studies of the Maillard reaction products of a protein using ion trap mass spectrometry. *Journal of Mass Spectrometry*, *35*(2), 131–138. https://doi.org/10.1002/(SICI)1096-9888(200002)35:2<131::AID-JMS920>3.0.CO;2-0

Tu, Z. cai, Zhong, B. zhen, & Wang, H. (2017). Identification of glycated sites in ovalbumin under freeze-drying processing by liquid chromatography high-resolution mass spectrometry. *Food Chemistry*, *226*, 1–7. https://doi.org/10.1016/j.foodchem.2017.01.038

Urisu, A., Kondo, Y., & Tsuge, I. (2015). Hen's Egg Allergy. *Chemical Immunology and Allergy*, *101*, 124–130. https://doi.org/10.1159/000375416

Wang, H., Sun, Q., Tan, J. ming, Hu, Y. ming, Yan, W., Li, Z., & Tu, Z. cai. (2020). Conformational alteration and the glycated sites in ovalbumin during vacuum freeze-drying induced glycation: A study using conventional spectrometry and liquid chromatography–high resolution mass

spectrometry. *Food Chemistry*, *318*, 126519. https://doi.org/10.1016/J.FOODCHEM.2020.126519

Yang, Y., Liu, G., & Wang, H. (2019). Investigation of the Mechanism of Conformational Alteration in Ovalbumin as Induced by Glycation with Different Monoses through Conventional Spectrometry and Liquid Chromatography High-Resolution Mass Spectrometry. *Journal of Agricultural and Food Chemistry*, *67*(11), 3096–3105. https://doi.org/10.1021/acs.jafc.8b06564

Declaration of interests

☒ The authors declare that they have no known competing financial interests or personal relationships that could have appeared to influence the work reported in this paper.

☐The authors declare the following financial interests/personal relationships which may be considered as potential competing interests:

Credit of Authors

Conceptualization and methodology: C.L., C.B., H.R. and D.T.; Formal analysis and investigation: M.C., W.D., D.T. and V.L.,; Data curation : M.C.; Writing _original draft preparation : M.C., W.D., and H.R.;

Journal Pre-proofs

Writing-review and editing, M.C., W.D., V.L., C.L, C.B., D.T., and H.R.; Supervision : H.R. and D.T.; Funding acquisition : H.R. and D.T.
All authors have read and agreed to the published version of the manuscript.

Highlights :

- Glycation and aggregation significantly lower the IgE binding capacity of OVA.
- Mass spectrometry unveils structural modifications induced by glycation and aggregation.
- Aggregation and glycation take place in and near known human IgE linear epitopes.
- Aggregation is driven by neo-formation of disulfide and dehydroprotein bridges.
- Aggregation masks epitopes of native OVA structure via bridging of inner residues.

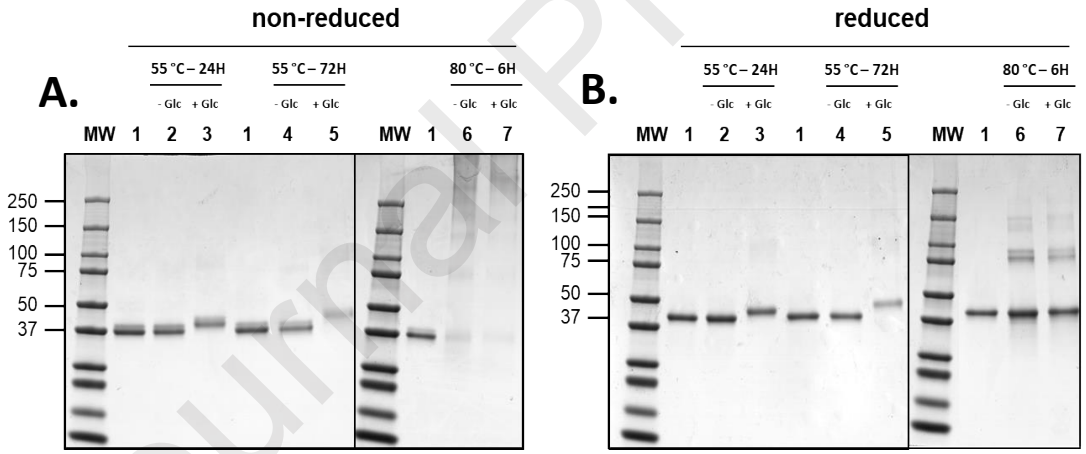

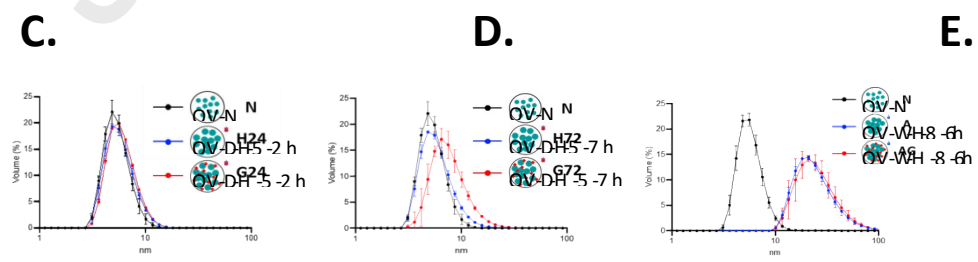

Journal Pre-proofs

Figure 1 : Structural analysis of modified OVA samples at protein level. A: SDS-PAGE profile of OVA samples in non reducing conditions (1: OVA-N ; 2: OVA-W-H-80-6h ; 3: OVA-W-HG-80-6h ; 4: OVA-D-H-55-24h ; 5: OVA-D-HG-55-24h ; 6: OVA-D-H-55-72h ; 7: OVA-D-HG-55-72h). **B:** SDS-PAGE profile of OVA samples in reducing conditions (1: OVA-N ; 2: OVA-W-H-80-6h ; 3: OVA-W-HG-80-6h ; 4: OVA-D-H-55-24h ; 5: OVA-D-HG-55-24h ; 6: OVA-D-H-55-72h ; 7: OVA-D-HG-55-72h). **C:** DLS curves of OVA-N (black line), OVA-D-H55-24h (blue line) and OVA-D-HG-55-24h (red line); **D:** DLS curves of OVA-N (black line), OVA-D-H-55-72h (blue line) and OVA-D-HG55-72h (red line); **E:** DLS curves of OVA-N (black line), OVA-W-H-80-6h (blue line) and OVA-W-HG-80-6h (red line).

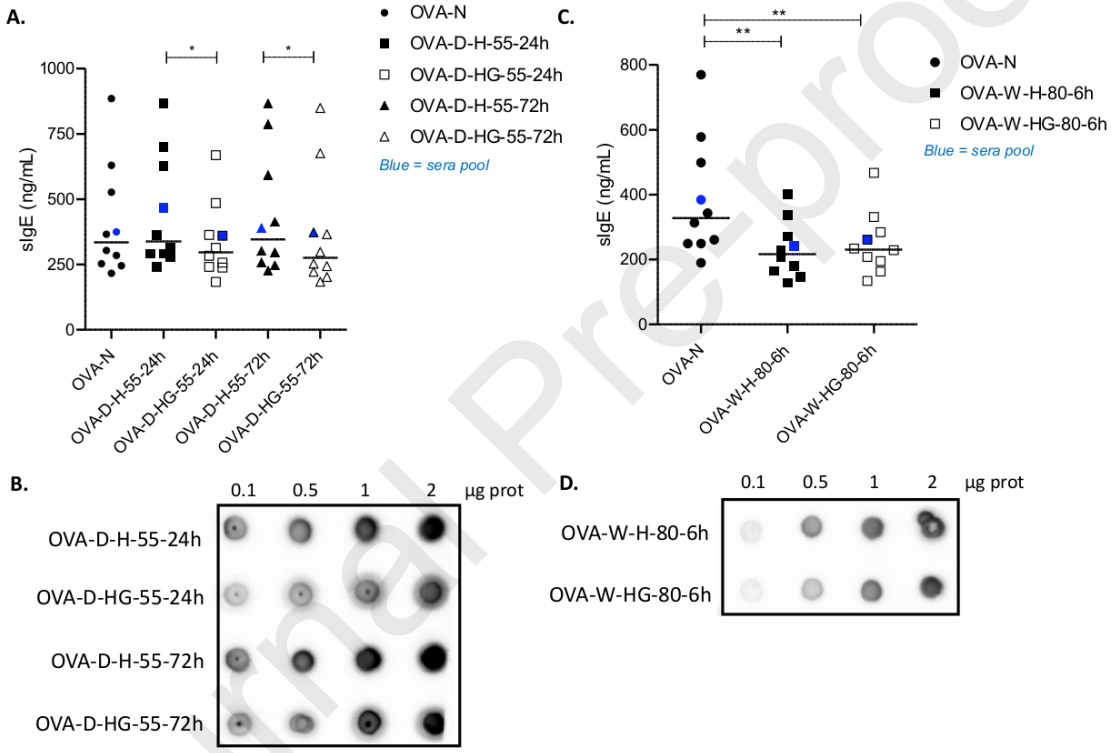

Figure 2: IgE binding capacity of different heated OVA samples, as determined using sera from egg-allergic patients. *A : Indirect ELISA using native OVA (OVA-N), 24h heated OVA at 55°C (OVA-D-H-55-24h), 24h heated OVA at 55°C in the presence of glucose (OVA-D-HG-55-24h), 72h heated OVA at 55°C (OVA-D-H-55-72h), 72h heated OVA at 55°C in the presence of glucose (OVA-D-HG-55-72h) with sera from egg-allergic individuals ; B : Dot Blot using native OVA (OVA-N), 24h heated OVA at 55°C (OVA-D-H-55-24h), 24h heated OVA at 55°C in the presence of glucose (OVA-D-HG-55-24h), 72h heated OVA at 55°C (OVA-D-H-55-72h), 72h heated OVA at 55°C in the presence of glucose (OVA-D-HG-55-72h) with sera from egg-allergic individuals ; C: Indirect ELISA using native OVA (OVA-N), heated & aggregated OVA at 80°C (OVA-W-H-80-6h), heated & aggregated OVA at 80°C (OVA-W-HG-80-6h) with sera from egg-allergic individuals ; D: Dot Blot using native OVA (OVA-N), heated & aggregated OVA at 80°C (OVA-W-H-80-6h), heated & aggregated OVA at 80°C (OVA-W-HG-80-6h) with sera from egg-allergic individuals*

Figure 2: IgE binding capacity of different heated OVA samples, as determined using sera from egg-allergic patients. A : Indirect ELISA using native OVA (OVA-N), 24h heated OVA at 55°C (OVA-D-H-55-24h), 24h heated OVA at 55°C in the presence of glucose (OVA-D-HG55-24h), 72h heated OVA at 55°C (OVA-D-H-55-72h), 72h heated OVA at 55°C in the presence of glucose (OVA-D-HG-55-72h) with sera from egg-allergic individuals ; B : Dot Blot using native OVA

(OVA-N), 24h heated OVA at 55°C (OVA-D-H-55-24h), 24h heated OVA at 55°C in the presence of glucose (OVA-D-HG-55-24h), 72h heated OVA at 55°C (OVA-D-H-55-72h), 72h heated OVA at 55°C in the presence of glucose (OVA-D-HG-55-72h) with sera from egg-allergic individuals ; C: Indirect ELISA using native OVA (OVA-N), heated & aggregated OVA at 80°C (OVA-W-H-80-6h), heated & aggregated OVA at 80°C (OVA-W-HG-80-6h) with sera from egg-allergic individuals ; D: Dot Blot using native OVA (OVA-N), heated & aggregated OVA at 80°C (OVA-W-H-80-6h), heated & aggregated OVA at 80°C (OVA-W-HG-80-6h) with sera from egg-allergic individuals

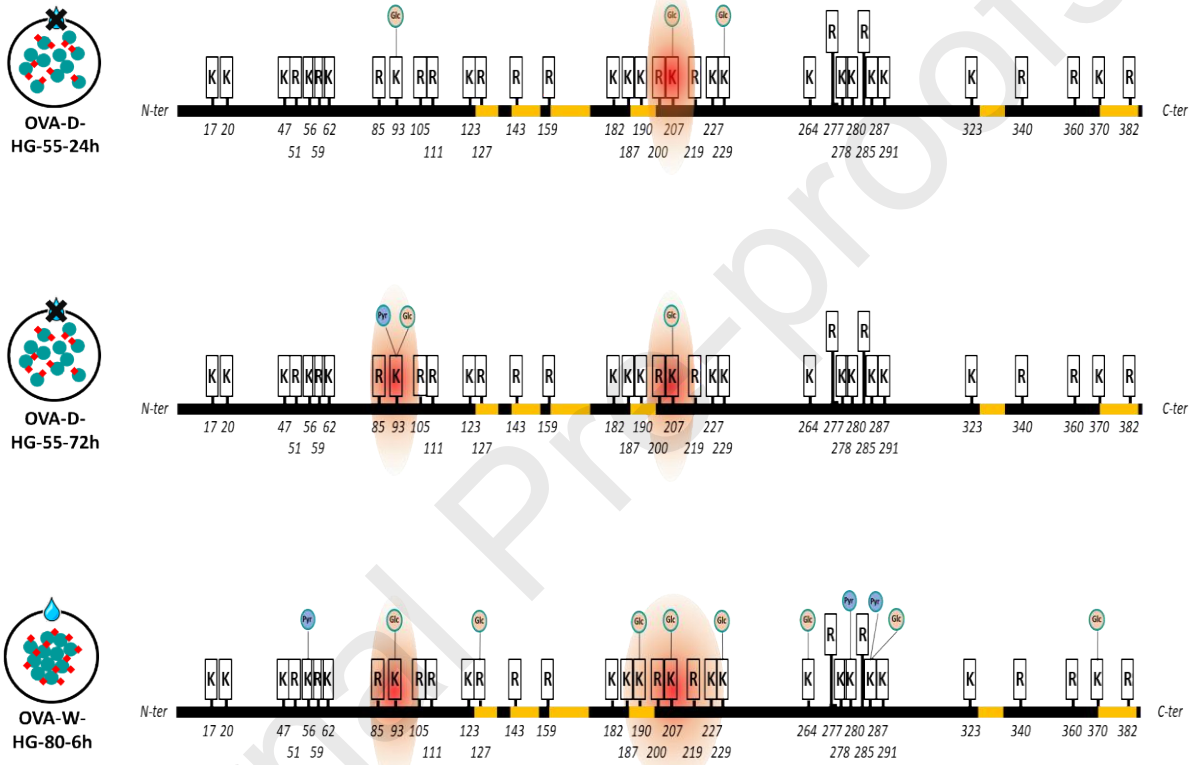

Fig 3 : Glycations sites localized on OVA linear sequence. Thick black bars represents the linearized primary sequence of OVA and all putative residues targeted by glycation (Lys and Arg) are pinned in boxes. Glycated residue are marked by orange and blue disks (Glc = Glucose adduct ; Pyr = Pyrraline adduct). Position of human IgE linear epitopes (according to Benedé et al., 2014) are positioned on OVA sequence as orange bars. Red ellipses represents the hotspot of aggregation determined by spectral counting of MS/MS spectrum attributed to each aggregation sites.

Journal Pre-proofs

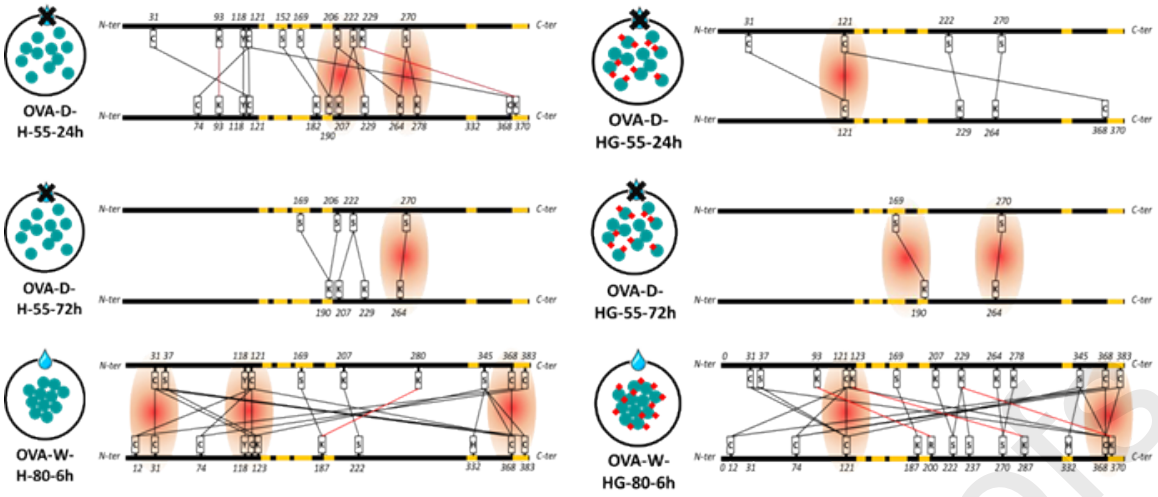

Figure 4 : Aggregation sites localized on OVA linear sequence. Thick black bars represents the linearized primary sequence of OVA with position of AA resiudes involved in bridges pinned in boxes. The black links between two residues indicate a bridge generated after heating and the red ones indicate a bridge generated after Maillard's reaction. Position of human IgE linear epitopes (according to Benedé et al., 2014) are positioned on OVA sequence as orange bars. Red ellipses represents the hotspot of aggregation determined by spectral counting of MS/MS spectrum attributed to each aggregation sites.

Table 1 : Number of MS/MS spectra attributed to OVA glycated peptides form according to type of adduct, amino acids involved and samples.

Type of adduct (induced deltaM in Da)	Glycated residue	Heating			Heating with glucose		
		In solution	Dry heating		In solution	Dry heating	
		6H	24H	72H	6H	24H	72H
Hexose (+162.0528)	K93	0	0	0	**31**	**6**	**18**
	K190	0	0	0	**18**	0	0
	K207	0	0	0	**43**	**15**	**25**
	K229	0	0	0	**23**	**7** 0	**9** 0
	K264	0	0	0	0		
	K287	0	0	0	**1**	0	0
	K370	0	0	0	**1**	0	0
	R127	0	0	0	**1**	0	0
Total		**0**	**0**	**0**	**127**	**28**	**43**

Pyraline (+108.021)	K56	0	0	0	**2**	0	0
	K93	0	0	0	*0*	0 **1**	
	K280	0	0	0	*1*	0 0	
	K287	0	0	0	**4**	0	0
Total		**0**	**0**	**0**	**7**	**0**	**1**

Table 2 : Number of MS/MS spectra attributed to OVA aggregated peptides form according to type of linker, amino acids involved in the bridge and samples.

Linker	Site 1	Site 2	Heating			Heating with glucose		
			In solution	Dry heating		In solution	Dry heating	
			6H	24H	72H	6H	24H	72H
diTyr	Y118	Y118	**10**	**2**	0	0	0	0
DOLD	K187	K280	**4**	0	0	0	0	0
DOLD	K229	K370	0	**2**	0	**1**	0	0
DOLD	K123	K287	0	0	0	**1**	0	0
Histidinoalanine	S345	H332	**1**	0	0	**3**	0	0
Lanthionine	S37	C121	**2**	0	0	**4**	0	0
Lanthionine	S345	C368	**2**	0	0	**3**	0	0
Lanthionine	S345	C121	**1**	0	0	**1**	0	0
Lanthionine	S37	C368	**1**	0	0	0	0	0
Lanthionine	S345	C383	**1**	0	0	0	0	0
Lysinoalanine	S270	K264	0	**63**	**37**	**3**	**6**	**4**
Lysinoalanine	S222	K207	**15**	**41**	**2**	**2**	0	0
Lysinoalanine	S206	K190	0	**23**	**8**	0	0	0
Lysinoalanine	S169	K187	**14**	0	0	**7**	0	0
Lysinoalanine	S169	K190	0	**2**	**2**	0	0	**4**
Lysinoalanine	S222	K229	0	**3**	**1**	**1**	**2**	0
Lysinoalanine	S270	K278	0	**1**	0	**4**	0	0
Lysinoalanine	S206	K264	0	**2**	0	0	0	0
Lysinoalanine	S37	K123	**1**	0	0	0	0	0
Lysinoalanine	S152	K182	0	**1**	0	0	0	0
Lysinoalanine	S237	K229	0	0	0	**1**	0	0
MOLD	K93	K93	0	**2**	0	0	0	0
Pentosidine	K93	R200	0	0	0	**2**	0	0
S-S	C121	C368	**42**	**2**	0	**40**	**7**	0
S-S	C31	C121	**27**	**5**	0	**13**	**6**	0

Journal Pre-proofs

S-S	C121	C121	**19**	**2**	0	**23**	**5**	0
S-S	C368	C368	**16**	0	0	**7**	0	0
S-S	C31	C368	**10**	0	0	**2**	0	0
S-S	C74	C121	**4**	**1**	0	**2**	0	0
S-S	C12	C121	**4**	0	0	**2**	0	0
S-S	C74	C383	**2**	0	0	**4**	0	0
S-S	C368	C383	0	0	0	**6**	0	0
S-S	C31	C31	**3**	0	0	0	0	0
S-S	C31	C383	**3**	0	0	0	0	0
S-S	C12	C368	**1**	0	0	**2**	0	0
S-S	C74	C368	0	0	0	**2**	0	0
Total			**183**	**152**	**50**	**136**	**26**	**8**

Journal Pre-proofs